PANEL FLUTTER ANALYSIS OF CURVED PANELS FOR LAUNCHER APPLICATIONS

Carrera E.[1], Zappino E.[1], Augello G.[2],Ferrarese A.[2],Montabone M.[2]
[1]POLITO, Politecnico di Torino, Aerospace Engineering Department, Italy.
[2]TASI, Thales Alenia Space Italia, Torino, Italy.

Abstract

The aeroelastic behavior of a Versatile Thermal Insulation (VTI) has been investigated. Among the various loadings acting on the panels in this work the attention is payed to fluid structure interaction. e.g. panel flutter phenomena. Known available results from open literature, related to similar problems, permit to analyze the effect of various Mach regimes, including boundary layers thickness effects, in-plane mechanical and thermal loadings, nonlinear effect and amplitude of so called limit cycle oscillations. Dedicated finite element model is developed for the supersonic regime. The model used for coupling orthotropic layered structural model with to Piston Theory aerodynamic models allows the calculations of flutter conditions in case of curved panels supported in a discrete number of points. Through this approach the flutter boundaries of the VTI-panel have been investigated.

1 Introduction

In the frame of the Cryogenic Upper Stage Technologies (CUST) development program part of the ESA Future Launcher Preparatory Program FLPP project (Prime of which is EADS-Astrium) the use of Versatile Thermal Insulation (VTI) panels has been proposed to protect the cryogenic tanks during the very early stage of the launcher flight.
VTI panels are attached at the upper stage of launcher for some dozens of seconds and then released by means of pyrotechnical separation nuts. The competitiveness of VTI solution with respect to existing and used upper stage structures must be checked carefully in order to make a proper decision for its use in future launcher.
In particular the success of VTI panel solution is very much subordinate to its lightness. The panels should be as light as possible but at the same time they must survive to the loadings acting on it during flight. Among the various loadings acting on the panels a particular attention is in this activities devoted to fluid structure interaction coupling sensitive loads, therefore an effort has been addressed focusing in the aero-elastic analyses and in particular in panel-flutter phenomena.
The panel flutter may appears during different Mach regimes. In the subsonic one it is called low frequency panel flutter and it apperas as a divergence phenomena. In the transonic and low supersonic range it appears as a single mode flutter, due to the flow non-liberaties it is mandatory to approach this problem with refined aerodynamic model such as Navier-Stokes model Hashimoto *et al.* [12]. In the supersonic regimes the panel flutter appear as coupled mode flutter; due to the aerodynamic forces two frequencies become closer and closer, when there is the coalescence usually the damping becomes positive and the flutter appears.
During the last fifty years many works on panel flutter have been proposed. Many efforts have been made during the sixties in order to develop a first approach to the problem. Some reviews have been presented by Dowell [5],Fung [9],Johns [13]. In these works some elementary approaches have been proposed based on the classical plate theory and on supersonic linear aerodynamic models like the piston theory [1]. The results concern simple geometry and simple boundary conditions (simply supported or clamped) along with analytical solutions available at that time.
Further improvements of the works just mentioned have been presented in the following years in order to extend the analyses to different geometries. Ganapathi [10] gave some results taking in to account the curvature; skew panels have been analyzed by Kariappa *et al.*

[14] that considered also the yawed angle of the flow. A comprehensive analysis of composite panels have been presented by Dixon and Mei [4] which introduced the effects of the orthotropy.
In the recent years some new developments have been proposed in order to overcome the problem related to the piston theory which ensure a good accuracy only for Mach number greater then 1.5 . Gordiner and Visbal [11] used a 3D viscid aerodynamic model coupled with a nonlinear structural model to study the transonic behavior of the panel flutter, taking in to account also the effects of the boundary layer. In the work by Hashimoto *et al.* [12] the effects of the boundary layer have been studied comparing the results from CFD analysis with those from a shear flow model proposed by Dowell [6].
Despite the number of work that has been presented on panel flutter, problems as the transonic analysis, boundary layer effects and 'non standard' boundary conditions have not been developed in all their features although these are critical in the design process.

2 Structural FE Model

The structural model introduced in this work is based on the Carrera Unified Formulation (CUF).
This section describes shorty the formulation in order to highlight the main features of the model from the mathematical point of view. A more comprehensive description may be found in the work by Carrera and Giunta [2], Carrera *et al.* [3].

Considering a three dimensional body it is possible to define a generic displacement field in the form:

$$s\left(x,y,z;t\right)=\left\{\begin{array}{c} u_x\left(x,y,z;t\right) \\ u_y\left(x,y,z;t\right) \\ u_z\left(x,y,z;t\right) \end{array}\right\} \tag{1}$$

In the Carrera Unified Formulation frameworks the displacement field is assumed do be the product of the cross section-deformation (approximate by a function expansion, F_τ) and the axial (y-direction) displacement, this assumption is summarized in the formulation:

$$\mathbf{s}\left(x,y,z;t\right)=F_\tau(x,z)\mathbf{s}_\tau(y,t), \quad \tau=1,2,....,M \tag{2}$$

where M stands for the number of terms of the expansion. There is no a unique choice of function $F_\tau(x,z)$, Lagrange polynomials are herein used to describe the cross-section displacement field, in the following analysis L9 elements will be used. Three-, L3, four-, L4, and nine-point, L9, polynomials can be adopted, in the following analysis L9 elements will be used.
Introducing the stress and strain relation in their classical form using the geometrical relations and the Hooke law:

$$\begin{array}{c} \epsilon_p=D_p\mathbf{s} \\ \epsilon_n=D_n\mathbf{s} \end{array} \tag{3}$$

and

$$\begin{array}{c} \sigma_p=\tilde{C}_{pp}\epsilon_p+\tilde{C}_{pn}\epsilon_n \\ \sigma_n=\tilde{C}_{np}\epsilon_p+\tilde{C}_{nn}\epsilon_n \end{array} \tag{4}$$

it is possible to derive the formulation of the internal strain energy by means of the Principle of Virtual Displacements:

$$\delta L_{int}=\delta L_{ext}=\int_V(\delta\epsilon_p^T\sigma_p+\delta\epsilon_n^T\sigma_n)dV \tag{5}$$

The solution of the aeroelastic model may be obtained in many ways. In this work a Finite element formulation is adopted to deal with arbitrary geometries, stacking sequence lay-out, boundary conditions, and loadings.
The FE formulation introduce a discretization on the longitudinal axis of the structure ($y-axis$). This approach allows to consider the unknown terms, $\mathbf{s}_\tau(y,t)$, reported in eq.2 as the product of an unknown constant, $q_{\tau i}$, and a known shape function, N_i.

$$\mathbf{s}\left(x,y,z;t\right)=F_\tau(x,z)N_i(y)q_{\tau i}(t), \quad i=1,2,....,N \tag{6}$$

Where N represent the number of nodes of the shape functions. The shape functions N_i may be chosen arbitrarily, in this work cubical Lagrange functions (B4, N=4) have been employed.

CUF allows to develop a finit element for any values of N and M without the need of an *ad hoc* formulation. For sake of brevity in the following sections only the main steps in the matrix derivation are reported.

2.1 Structural stiffness matrix [K]

The structural stiffness matrix can be written starting from the internal energy equation; substituting eq.6 in eq.3 and 4 is possible to reduce the eq.5 in the following form:

$$L_{int} = \delta \mathbf{q}_i^T \Big[\int_l f(N_i, N_j) dy \cdot \int_\Omega g(F_\tau, F_s, D_p, D_n, \tilde{C}) d\Omega \Big] \mathbf{q}_j \tag{7}$$

Where f is function only of the longitudinal axis coordinate (y), and g is function of the cross-section (Ω) coordinates (x ,z). The final compact formulation of the stiffness matrix is:

$$L_{int} = \delta \mathbf{q}_i^T \left[K^{ij\tau s} \right] \mathbf{q}_j \tag{8}$$

2.2 Structural mass matrix [M]

The mass matrix formulation derive from the inertial energy that can be written in the following formulation:

$$L_{inerz} = \int_V (\delta \mathbf{s} \cdot \ddot{\mathbf{s}} \cdot \rho(x, z)) dV \tag{9}$$

Substituting eq. 6 in eq. 9 the inertial energy assume the formulation:

$$\delta L_{inerz} = \delta \mathbf{q}_{i\tau}^T \Big[\int_V (F_\tau \cdot N_i \cdot N_j \cdot F_s \cdot \rho(x, z)) dV \Big] \ddot{\mathbf{q}}_{sj} = \delta \mathbf{q}_{i\tau}^T \left[M^{ij\tau s} \right] \ddot{\mathbf{q}}_{sj} \tag{10}$$

The mass matrix [M] so is function of the shape function of N_i, F_τ and of the density ρ that may be not constant on the cross section, ρ(x,z).

3 Aerodynamic Model

As first approach in the VTI-panel aeroelastic analysis a linear quasi-static model has been chosen, in particular in the present work is used the model introduced by Lightill [18] and Ashley and Zartarian [1] called *piston theory*.
The piston theory has been widely employed in the panel flutter analyses because of its simple formulation and its good accuracy in the supersonic flow. Despite this, it is important to underline the lacks of the piston theory formulation:

- it can't detect single mode panel flutter and divergence;
- it provides a good accuracy only for Ma greater than 1.5;
- it considers a inviscid linear flow, so the boundary layer effects are not considered.

The piston theory assumes the flow on a panel to be similar to an one-dimensional flow in channel (in a piston). Generally speaking the pressure acting on the panel may be expressed in the form reported in eq.11.

$$\Delta p(x, t) = \frac{2q}{\sqrt{M^2 - 1}} \Big\{ \frac{\delta w}{\delta y} + \frac{M - 2}{M - 1} \frac{1}{V} \frac{\delta w}{\delta t} \Big\} = A \frac{\partial w}{\partial y} + B \frac{\partial w}{\partial t} \tag{11}$$

The complete derivation of this formulation can be found in the work by Van Dyke [21],[18]. Eq.11 shows that the local pressure is function of the velocity (V), the Mach number (M), of the normal displacement (w) and of the slope of the surface ($\partial w / \partial y$).

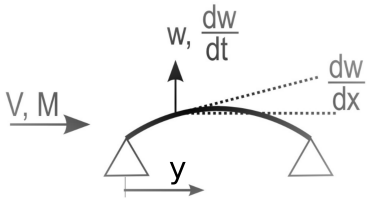

Figure 1: Piston theory system of reference.

3.1 Aerodynamic matrices [K_a] and [D_a]

The aerodynamic matrix may be derived evaluating the work,$\delta L_{\delta s}^{\Delta p}$, of a differential pressure, Δp, acting on a surface, Λ.

$$\delta L_{\delta s}^{\Delta p} = \int_{\Lambda} (\delta \mathbf{s} \Delta p)\, d\Lambda \tag{12}$$

In the case of piston theory the differential pressure may be described by means of eq. 11. In the CUF frameworks and using a FE approach the differential pressure assumes the formulation:

$$\Delta p = A\frac{\partial w}{\partial y} + B\frac{\partial w}{\partial t} = AI_{\Delta p} q_{i\tau} F_\tau \frac{\partial N_i}{\partial y} + BF_\tau N_i I_{\Delta p} \frac{\partial q_{i\tau}}{\partial t} \tag{13}$$

Where:

$$I_{\Delta p} = \begin{bmatrix} 0 & 0 & 0 \\ 0 & 1 & 0 \\ 0 & 0 & 0 \end{bmatrix} \tag{14}$$

Upon substituting eq.13 in eq.12 the following variational formula can be derived:

$$\delta L_{\delta s}^{\Delta p} = \int_{\Lambda} \delta q_{i\tau} F_\tau N_i \big(AI_{\Delta p} q_{sj} F_s \frac{\partial N_j}{\partial y} + BF_\tau N_i I_{\Delta p} \frac{\partial q_{sj}}{\partial t} \big)\, dx\, dy = \delta q_{i\tau}^T \big[\mathbf{K}_a^{ij\tau s}\big] q_{sj} + \delta q_{i\tau}^T \big[\mathbf{D}_a^{ij\tau s}\big] \frac{\partial q_{sj}}{\partial t} \tag{15}$$

Where $\big[\mathbf{K}_a^{ij\tau s}\big]$ is the aerodynamic stiffness matrix and may be written in the form:

$$\big[\mathbf{K}_a^{ij\tau s}\big] = A \int_x \big(F_\tau F_s\big)\, dx \begin{bmatrix} 0 & 0 & 0 \\ 0 & \int_L N_i \frac{\partial N_j}{\partial y}\, dy & 0 \\ 0 & 0 & 0 \end{bmatrix} \tag{16}$$

and $\big[\mathbf{D}_a^{ij\tau s}\big]$ is the aerodynamic damping matrix and it may be written in following form:

$$\big[\mathbf{D}_a^{ij\tau s}\big] = B \int_x \big(F_\tau F_s\big)\, dx \begin{bmatrix} 0 & 0 & 0 \\ 0 & \int_L N_i N_j\, dy & 0 \\ 0 & 0 & 0 \end{bmatrix} \tag{17}$$

4 VTI-panel: a challenging problem

The VTI panels are a part of a larger structure which acts as thermal protection of an internal tank, the whole structure is divided into six panels, each of them has the same geometry. The characteristic dimensions are collected in Tab. 1.

Panel lenght	a	[m]	2.52
Panel width	b	[m]	2.71
Curvature radius	R	[m]	2.79
Thickness	t	[m]	0.02132

Table 1: Physical dimensions of the VTI panel.

Each panel is pinched in 4 points, close to the corner, and it is connected (in the longitudinal direction) to the adjacent panels with correspondence to half length of the panel $a/2$.

4.1 Material

The VTI panels are made of a sandwich structure. The material is composed by means of a light core, see Fig. 2, which is denoted as material 1 (Mat. 1) and covered by two thin skins built by 4 layers. Each layer is made of two different materials indicated as Mat. 2 and Mat. 3. The properties of each layer are classified.

Id. Layer	Material	Thickness $[m] \times E-4$	Orientation $[deg]$
1	Mat. 3	2.0	45
2	Mat. 2	1.3	0
3	Mat. 2	1.3	0
4	Mat. 3	2.0	45
5	Mat. 1	200	0
6	Mat. 3	2.0	45
7	Mat. 2	1.3	0
8	Mat. 2	1.3	0
9	Mat. 3	2.0	45

Table 2: VTI panel: Lamination parameters.

4.2 Mission Profile

From the available data of the Launcher [[7], [19]] it is possible to define a characteristic mission profile in which the VTI panels will be involved in terms of Mach number and static pressure. In the aircraft design the panel flutter phenomena is analyzed considering a flow with constant parameters, the critical conditions are investigated changing the flight speed. This approach is suitable for an aircraft flying at a constant altitude. The VTI-panels problem can't be studied with the classical approach described above because the flow parameters are time-dipendent because the altitude changes during missiles flight. In eq. 11 the aero-

Times $[s]$	*Altitude* m	*Mach*	P_{atm} $[Pa]$	ρ $[Kg/m^3]$	T K
36	2300	0.70	76157	0.976	273.0
41	3300	0.80	67760	0.881	266.5
47.5	4800	0.95	55071	0.752	256.8
51.5	5900	1.05	47562	0.667	249.6
56	7500	1.20	38226	0.557	239.2
63	9800	1.50	27332	0.423	224.3
72	12900	2.00	16722	0.270	216.5
84	18200	2.70	7208	0.117	216.5

Table 3: Flow

dynamic actions are function of the terms A and B, the former is related to the aerodynamic stiffness, the latter is a damping factor. In fig.2 the time evolution of the constants, A and B

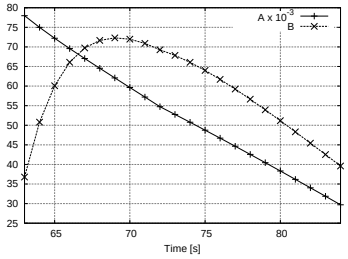

Figure 2: Piston theory costant.

from eq.11, of the piston theory in the supersonic regime are depicted over the whole supersonic range. The stiffness parameter, A, decreases during the whole Mach range because

of the reduction of the flow density. The damping factor has a maximum at 69 second, the growing part is due to the effects of the Mach growth, the second part is dominated by the density reduction. Both the coefficients become smaller and smaller increasing the time because of the reduction of the density, therefore the aerodynamic effects are stronger in the first part of the flight.
In literature there are no works dealing with a problem similar to VTI-panels so a new approach has to be developed to make a proper panel flutter evaluation.

5 Remark on literature Results

In the last sixty years many works have been presented on panel flutter, in tab. 4 are summarized some of the valuable results. The effect of many parameter has been take into account: the aspect ratio (a/b), the curvature (R), the orthitropy (E_{11}/E_{22}), the differential pressure (Δp); the temperature (ΔT); the buckling load (P_{cr}) and the boundary layer thickness (δ).
For each features, if known, it is indicated the effects on the three characteristic parameter: q_f, f_f and h_f/t. An upper arrow ($\uparrow$) indicates that the features is directly proportional with the parameter while a down arrow ($\downarrow$) indicates that the features is inversely proportional to the parameter. If the information is no available an empty space is reported. The references and some comments are reported in the last columns.

Features	q_f	f_f	h_f/t	References	Comments
$a/b \uparrow$	$\uparrow$	$\uparrow$	$\downarrow$	[5]	a constant
$R \uparrow$	$\downarrow$	$\uparrow$		[10];[5]	
$\frac{E_{11}}{E_{22}} \uparrow$	$\uparrow$	$\uparrow$	$\downarrow$	[20]; [4];[15]	E_{22} constant
$\Delta p \uparrow$	$\uparrow$			[5]	
$\Delta T \uparrow$	$\downarrow$		$\uparrow$	[22];[17]	
$P_{cr} \uparrow$	$\downarrow$		$\uparrow$	[14];[5]	
$\delta \uparrow$	$\uparrow$	$\uparrow$	$\downarrow$	[11];[12]; [6]	

Table 4: Panel flutter parameter influence

Starting from the results above and by considering the geometry of the VTI panel it is possible to make some preliminary evaluation on the panel aeroelastic stability. Because of the lack of results in the literature for panels with the same features of VTI the following consideration are related to a panel with similar geometrical features and for simply supported boundary conditions. The results are reported in terms of critical dynamic pressure, $P_{dyn_{CR}}$, compared with the pressure acting on the panel, $P_{tot_{Max}}$.

$times$	$Mach$	$P_{tot_{Max}}$	$P^{flat}_{dyn_{CR}}$	$P^{curved}_{dyn_{CR}}$
56	1.20	58840	170624	454998
63	1.50	42485	234608	625622
72	2.00	28848	615669	1641786
84	2.70	12357	917035	2445426

Table 5: Effects of the curvatures on critical dynamic pressure by Ganapathi [10].(Simply supported panel).

$times$	$Mach$	$P_{tot_{Max}}$	$P^{Kariappa}_{dyn_{CR}}$	$P^{Laurenson}_{dyn_{CR}}$
56	1.20	58840	158778	141780
63	1.50	42485	218319	244990
72	2.00	28848	572922	445630
84	2.70	12357	853363	644590

Table 6: Comparisons between results from Kariappa *et al.* [14] and Laurenson and Mcpherson [16] .

In tab.5 are reported the results for a isotropic panel in a flat and curve configurations evaluated by means of the work by Ganapathi [10].

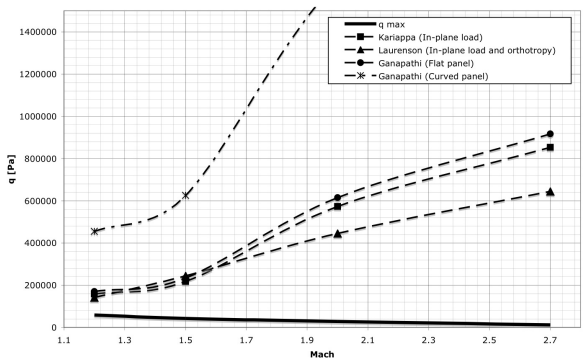

Figure 3: Comparisons of the flutter boundaries evaluated by means of different approach.

Tab.6 shows the comparisons between the results by Kariappa *et al.* [14] (flat isotropic panel with in-plane loads) and those by Laurenson and Mcpherson [16] (flat orthotropic panel with in-plane loads).
In fig.3 all the results are compared with the mission profile. It is clear that the $P_{tot_{Max}}$, the solid line, is always lower than the critical pressure.
Is important to remark that this results are for a simply supported condition. Because of the results by Fan and Cheung [8], that shows the great influence of the pinched boundary condition on the natural frequency, a FE model have been developed in order to investigate the panel flutter boundaries on the real structure.

6 FE model Results

6.1 Panel Baseline Analyses Results

A comprehensive panel flutter analysis is presented in this section. Many Model have been take into account in order to give a complete overview of the aeroelastic behavior of the VTI-panel and to describe the effects of the geometric parameter and boundary condition. In fig.5 the different models are depicted. The evolution of the natural frequencies along the whole supersonic range have been considered for each model considered. The instabilities have been detected looking for positive value of dumping factor.
In fig.4 are reported the results for the model C2 (Curved panel with four pinched corner). In the first part of the mission profile the second and the third modes are coupled in an aeroelastic instability. This condition lasts up to the second 65.5 when the unstable branch of the damping factor from positive (unstable - ◯) turns in negative (stable - •). The coalescence of the frequencies lasts up to second 67.8 when they splint into to different modes. In fig. 5

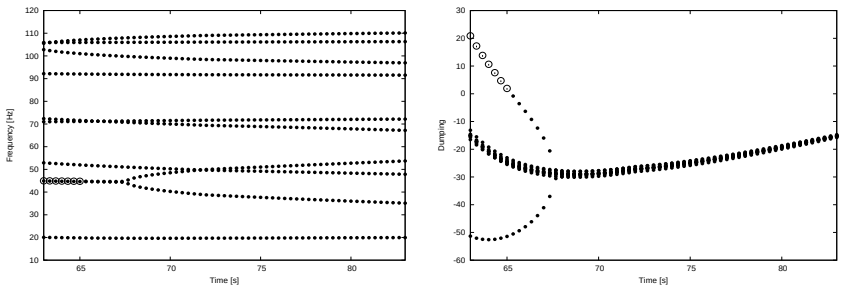

Figure 4: Time evolution of the natural frequencies and damping factor. Model C2. (•) Stable;(◯) Unstable.

the results are summarized of the whole considered cases. The results show that the two model simply supported, Mod.F1 an Mod.C1, are stable along the whole supersonic range (solid line). The Mod.F1 if always instable (dashed line), but, if it is considered the curvature, Mod.C2, it becomes stable in the second part of the supersonic range. In the Mod.C3 two additional constrains have been introduced in order to analyze the effects of connection between the panels. The VTI-panel configuration is the one closer to Mod.C2 because the

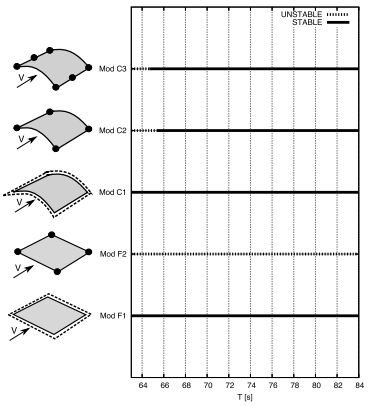

Figure 5: Stability range summary.(– – – –) Simply supported; (•) Piched.

Mod.C3 is non enough conservative (the connections can not be considered as rigid constraints)
The results show that the model is critical in the first part of the supersonic regimes, so, **the panel configuration seems non suitable for the mission profile.**
In fig.6 at every time step has been evaluated the critical Mach of each model.

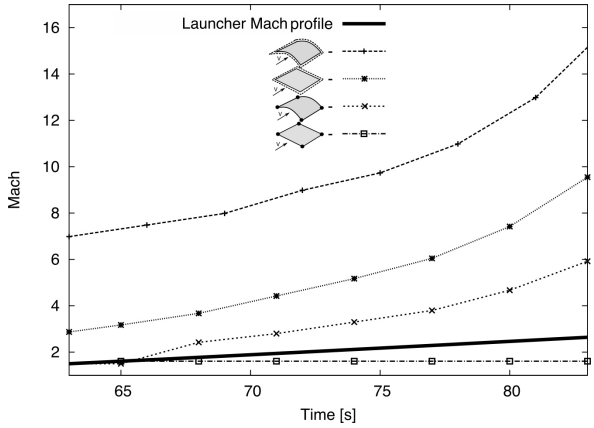

Figure 6: Stability margin of considered models.(– – – –) Simply supported; (•) Piched.

6.2 Panel Design Improvement

Because of the results reported below the VTI-panel model needs a redesign process in order to look for possible improvement of aeroelastic response in the supersonic regime. Two different solution have been considered:

- to modify boundary condition;
- to increase the stiffness by increasing the thickness of the sandwich panel faces.

Many different boundary condition configuration are shown in fig.7. The results show that all the new solutions herein proposed (from Mod.C4 to Mod.C8) make the panel stable during the whole supersonic regime. To have more informations about the effects of the boundary conditions on the flutter boundaries it is useful to analyze the flutter margins reported in fig. 8.]] From the results it seems that the solution Mod.C9 is one of the more efficient because makes the panel stable introducing only one more pinched constrains in the middle of the trailing edge.

The second approach in the redesign analysis is to change the geometrical properties of the panels. A preliminary study has been carried out changing the thickness of the layers. The optimization has been carried out on Mod.C2. This case, in fact, matches with the VTI-panel features. Tab.7 shows the lamination properties used in the redesign process. A

Figure 7: Flutter range of the redesigned models.

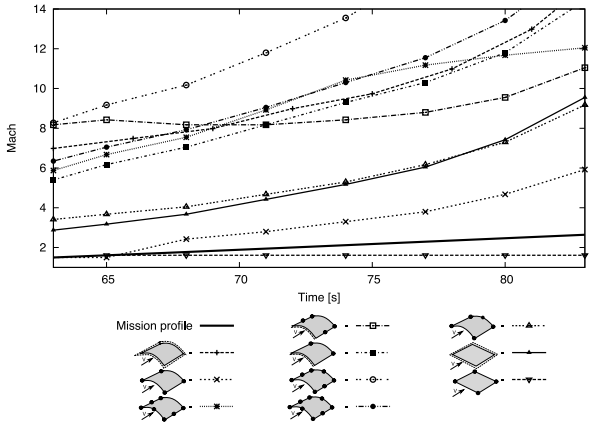

Figure 8: Flutter margin of the redesigned models.

Id. Layer	Material	Thickness $[m] \times E - 4$	Orientation $[deg]$
1	Mat. 3	$2.0 \times \xi$	45
2	Mat. 2	$1.3 \times \xi$	0
⋮	⋮	⋮	⋮
8	Mat. 2	$1.3 \times \xi$	0
9	Mat. 3	$2.0 \times \xi$	45

Table 7: Parameters used to redesign the VTI panel.

new parameter , ξ, have been added. It has been called thickness ration and it acts on the thickness of the two outer layers. For ξ equal to one the panel is in the standard configuration, if ξ is lower than one the thickness is reduced, otherwise, for ξ bigger than one it is increased. Fig. 9a shows the stability range for different value of ξ. Increasing the thickness of the outer layer the stable region is extended. For ξ=1.5 the panel is stable on the whole supersonic range. The same results may be observed in fig.9b where the critical Ma has been reported. Increasing the parameter ξ the critical Ma became bigger and bigger. For ξ=1.5 the critical

Ma is bigger than the design Ma at each time step, so the panel is stable.

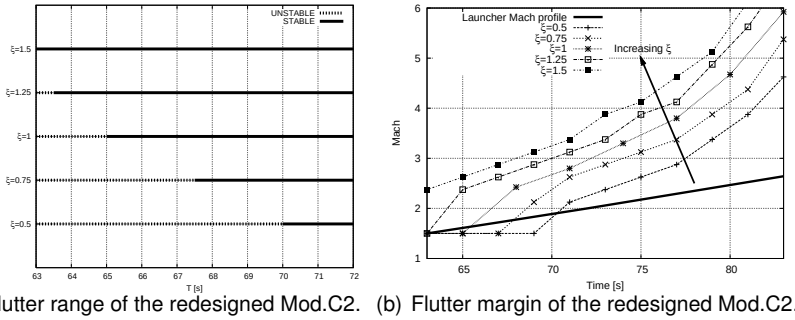

(a) Flutter range of the redesigned Mod.C2. (b) Flutter margin of the redesigned Mod.C2.

Figure 9: Performances of redesigned Mod.C2 VTI-panels for different ξ values.

Some considerations may be made about the effects of the variation of ξ on the weight of the panel. Fig. 10a shows the relation between ξ and the weight increment. The results

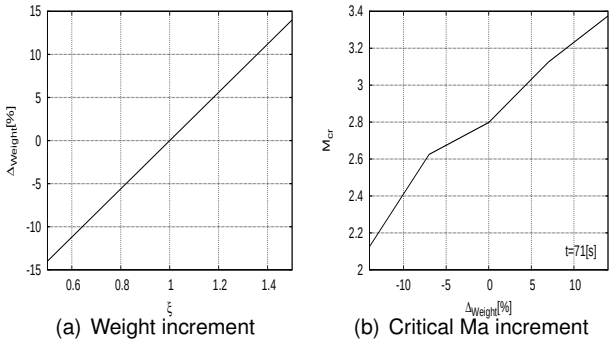

(a) Weight increment (b) Critical Ma increment

Figure 10: Effects of the stiffness redesign on VTI-panel weight.

show that to make the VTI-panel stable by means of the parameter ξ the weight has been increased of 14%. In fig.10b the weight increment is related to the critical Ma at t=71[s].
From the results presented in this section the following statements hold:

- it is possible to improve the critical Ma by changing the boundary condition without increase the panel weight;
- the panel faces thickness has a strong influence on the stability region but also on the weight of the panel.

7 Conclusions

From the results of the VTI-panel carried out in the FE analysis the panel shows an aeroelastic instability in the first part of the supersonic range (from t=63[s] up to t=65.5[s]). These results suggest a redesign process of the VTI-panel in order to avoid the critical conditions.
Two different redesign approaches have been proposed. The first suggests to change the constrains configuration. Many different settings have been considered and it was possible to make the panel stable on the whole supersonic range. In the second redesign approach the thickness of the face of the sandwich panel has been changed. In conclusion, by means of this approach, not only the flutter boundaries have been investigated, but many redesign solution have been proposed in order to increase the flutter boundaries without affect significantly the configuration and weight of the launcher.
By taking into account what above and to extend the analysis at subsonic and transonic ranges the following two points appear of interest for future developments: (1) A complete aeroelastic analysis based on CFD approaches in the transonic and low supersonic range ($0.7 < M < 0.1.5$) including boundary layer influence and transonic phenomena; viscid and inviscid case should be investigated; (2) Experiment and wind tunnel test could results extremely useful to assess computational aeroelastic tools.

Acknowledgment

The Regione Piemonte project MICROCOST is gratefully acknowledged for the financial support

References

[1] Ashley, H. and Zartarian, G. (1956). Piston theory - a new aerodynamic tool for the aeroelastician. *Composites Structures*, pages 1109–1118.

[2] Carrera, E. and Giunta, G. (2010). Refined beam theories based on a unified formulation. *International Journal of Applied Mechanics*, **2**(1), 117–143.

[3] Carrera, E., Giunta, G., Nali, P., and Petrolo, M. (2010). Refined beam elements with arbitrary cross-section geometries. *Computers and Structures*, **88**(5–6), 283–293. DOI: 10.1016/j.compstruc.2009.11.002.

[4] Dixon, I. R. and Mei, C. (1993). Finite element analysis of large-amplitude panel flutter of thin laminates. *AIAA Journal*, **31**, 701–707.

[5] Dowell, E. H. (1970). Panel flutter: A review of the aeroelastic stability of plates and shell. *AIAA Journal*, **8**, 385–399.

[6] Dowell, E. H. (1973). Aerodynamic boundary layer effects on flutter and damping of plates. *Journal of Aircraft*, **8**, 734–738.

[7] EADS-ASTRIUM (2010). Cust2-ast-tn-01-0001. Technical report, EADS ASTRIUM.

[8] Fan, S. C. and Cheung, Y. K. (1984). Flexural free vibration of rectangular plates with complex support conditions. *Journal of Sound and Vibrations*, **93**, 81–94.

[9] Fung, Y. C. B. (1960). A summary of the theories and experiments on panel flutters. *AFOSR-TN-60-224*, **8**, 734–738.

[10] Ganapathi, M. (1995). Supersonic flutter of laminated curved panels. *Defense Science Journal*, **45**, 147–159.

[11] Gordiner, R. E. and Visbal, M. R. (2002). Development of a three-dimensional viscous aeroelastic solver for nonlinear panel flutter. *Journal of Fluids and Structures*, **16**, 497–527.

[12] Hashimoto, A., Aoyama, T., and Nakamura, Y. (2009). Effects of turbulent boundary layer on panel flutter. *AIAA Journal*, **47**, 2785–2791.

[13] Johns, D. J. (1965). A survey on panel flutter. *AGARD-AR-1*.

[14] Kariappa, B., Komashekar, B. R., and Shah, C. G. (1970). Discrete element approach to flutter of skew panels with in-plane forces under yawed supersonic flow. *Journal of Sound and Vibrations*, **8**, 2017–2022.

[15] Kouchakzadeh, M. A., Rasekh, M., and Haddadpoura, H. (2010). Panel flutter analysis of general laminated composite plates. *Composites Structures*, **92**, 1906–2915.

[16] Laurenson, R. M. and Mcpherson, J. I. (1977). Design procedures for flutter-free surfacepanels. *NASA-CR-2801*.

[17] Lee, I., Lee, M. D., and Ho, K. (1999). Supersonic flutter analysis of stiffened laminates plates subject to thermal load. *Journal of Sound and Vibrations*, **229**, 49–67.

[18] Lightill, M. J. (1953). Oscillating airfoil at high mach number. *Journal of the Aeronautical Science*, **20**, 402–406.

[19] Müller, M. (2009). Cust-astrium-mmo-013. Technical report, EADS ASTRIUM.

[20] Shiau, L. C. and Lu, L. T. (1992). Nonlinear flutter of two-dimensional simply supported symmetric composite laminated plates. *Journal of Aircraft*, **29**, 140–145.

[21] Van Dyke, M. D. (1952). Study of second-order supersonic flow theory. *NACA Report 1081*.

[22] Xue, D. Y. and Cheung, Y. K. (1993). Finite element nonlinear panel flutter with arbitrary temperatures in supersonic flow. *AIAA Journal*, **31**, 154–162.